

iTRAQ-based quantitative proteomic analysis of defense responses of two tea cultivars to *Empoasca onukii* Matsuda feeding

Ruirui Zhang¹, Yueyue Tian², Xiaoyue Lun¹, Yan Cao¹, Xiangzhi Zhang¹, Meina Jin¹, Feiyu Guan¹, Liping Wang¹, Yunhe Zhao^{1*} and Zhengqun Zhang^{1*} 

¹ Shandong Agricultural University, Tai'an 271018, China

² Shandong University of Aeronautics, Bin'zhou 256600, China

* Corresponding authors, E-mail: yhzhao@sdau.edu.cn; zqzhang@sdau.edu.cn

Abstract

Empoasca onukii Matsuda is a pest which severely damages tea plants. In this study, an isobaric tag for relative and absolute quantitation (iTRAQ)-based quantitative proteomic analysis was performed to compare the leaves of two tea cultivars 'Huangjinya' and 'Fudingdabaicha' after *E. onukii* feeding. qRT-PCR was used to detect the gene expression levels of tea plants feeding by *E. onukii* with different population densities. The results showed that there were 168,983 specific spectra, 31,292 specific peptides, and 8,901 proteins being identified in 'Huangjinya' and 'Fudingdabaicha'. Psf and LHCA1 in Photosystem I were induced to be down-regulated in 'Huangjinya' under *E. onukii* infestation. In the lignin biosynthesis pathway, LAC1, LAC3, and POD1 were up-regulated significantly and POD11 was down-regulated in 'Huangjinya'. POD1 was up-regulated 2.01-fold in 'Huangjinya' and 1.73-fold in 'Fudingdabaicha' compared to the control. The qRT-PCR results showed several genes, such as *CsLAC2*, *CsCCR1*, *CsCCR2*, *CsCAD1*, and *CsCAD3* showed a trend of increasing, then decreasing and then sharply increasing expression in the low-density *E. onukii*-infested tea plant treatments. The results suggested that proteins involved in photosynthesis, such as PHCs, FNRs, and LHCs, showed down-regulation and proteins involved in lignin biosynthesis, such as PODs, CADs, and LACs, were upregulated in response to infestation by *E. onukii*. Through the changes in lignin synthesis-related genes, we hypothesized that there was a 'stress response-adaptation-defense response' process in the tea plants under *E. onukii* infestation. Our results provide insights into the dynamics and molecular mechanisms of two tea cultivars against *E. onukii* infestation.

Citation: Zhang R, Tian Y, Lun X, Cao Y, Zhang X, et al. 2023. iTRAQ-based quantitative proteomic analysis of defense responses of two tea cultivars to *Empoasca onukii* Matsuda feeding. *Beverage Plant Research* 3: e006 <https://doi.org/10.48130/bpr-0023-0039>

Introduction

Plants are subjected to biotic stresses including damage caused by insect pests during different periods of their growth. Biotic stresses trigger a series of plant defense responses: first perception of stress, then activate signaling pathways and alter gene expression levels, and consequently alter plant physiology, growth and development^[1]. Plant defense mechanisms against herbivorous pests include both direct and indirect defenses. Direct defense mechanisms include the change of plant characteristics that provide mechanical protection against further feeding of herbivores and the production of herbivore toxic or deterring alkaloids. Indirect defenses refer to the release of volatile organic compounds as the signals attracting parasitoids and predators of the herbivores^[2, 3].

Phenylpropanoid metabolism is one of the most important secondary metabolic pathways involved in plant defense against biotic stresses, and lignin synthesis is one of the branches of the phenylpropanoid pathway^[4,5]. Phenylalanine form three 4-hydroxyphenylpropanoids known as monolignols, p-coumaryl alcohol, coniferyl alcohol and sinapyl alcohol (termed monolignols), through a series of hydroxylation, methylation, ligation and reduction^[6,7]. Lignin is a complex and irregular biopolymer which is primarily derived from the polymerization of three monolignols, and provides mechanical strength and makes plant cell walls more difficult for piercing-sucking herbivores to penetrate and leaf-eating herbivores to

digest^[8, 9]. Multiple enzymes and their genes regulate plant lignin synthesis pathways. Lignin biosynthesis in plants begins with three consecutive reactions usually considered as the general phenylpropanoid pathway. The core three reactions are each catalyzed by phenylalanine ammonia lyase (PAL, EC 4.3.1.5), cinnamate-4-hydroxylase (C4H, EC 1.14.13.11), and 4-coumarate coenzyme A ligase (4CL)^[10]. Cinnamoyl-CoA reductase (CCR, EC 1.2.1.44) and cinnamyl alcohol dehydrogenase (CAD, EC 1.1.1.195) are the key enzymes in the lignin monomer synthesis pathway. CCR is an important enzyme in monolignol biosynthetic pathway and catalyzes the conversion of cinnamoyl CoA esters to their corresponding cinnamaldehydes, which is the first step in the lignin-specific branch of the phenylpropanoid pathway^[11]. CAD is responsible for the conversion of cinnamyl aldehydes to cinnamyl alcohols^[12]. The peroxidases (POD, E.C. 1.11.1.7) and laccases (LAC, EC 1.10.3.2) are potentially involved in the oxidation of lignin precursors in plant cell walls, which is the final step in lignin biosynthesis^[13,14]. Many genes related to phenylpropanoid metabolism and lignin synthesis were significantly activated after the plants were damaged by insect feeding^[15].

Tea plant *Camellia sinensis* (L.) O. Kuntze is an economically important evergreen woody crop, which has been grown in different agroclimatic zones to produce nonalcoholic beverages^[16–18]. As an evergreen woody plant, *C. sinensis* is susceptible to various biotic stressors such as pests and diseases, which

frequently cause tea yield losses^[19]. In Chinese tea plantations, *C. sinensis* is often exposed to biotic stresses from high populations of tea pests including the tea green leafhopper *Empoasca onukii* Matsuda^[20]. *E. onukii* is one of the most common and economically important piercing-sucking herbivores of *C. sinensis* and generally occur in 9–11 overlapping generations throughout the growing season of *C. sinensis*^[21,22]. Adults and nymphs suck the sap of tender shoots and buds, causing leaf edge yellowing, reddened veins, and wrinkled leaves^[23]. Tian founded that *E. onukii* infestation increased the thickness of xylem of tea shoots of two tea cultivars 'Huangjinya' and 'Fudingdabai'^[16]. Even though the morphological changes have been found to play roles in defense responses of *C. sinensis* against *E. onukii*, the fundamental mechanism of gene regulations by which tea plants protect themselves from *E. onukii* is still unclear.

Proteomics has rapidly developed, which has become a widely accepted method to study many species^[24,25]. The application of the isobaric tags for relative and absolute quantitation (iTRAQ) has led to critical developments in proteomics^[26,27]. In our previous study, the morphological, physiological and biochemical changes of different tea varieties 'Huangjinya' and 'Fudingdabai' after *E. onukii* infestation were determined, to determine the tolerance of different tea varieties to *E. onukii*. In general, the photobleaching cultivar 'Huangjinya' was susceptible to *E. onukii*, while 'Fudingdabai' was resistant to *E. onukii*^[16]. On the basis of our previous study, the iTRAQ comparative proteomic approach was employed to evaluate proteomic profile differences in two tea cultivars 'Huangjinya' (abbreviated as 'HJY') and 'Fudingdabaicha' (abbreviated as 'FDDB') after *E. onukii* feeding. These proteomic data are not only a valuable source for future identification of genes associated with resistance to *E. onukii*, but also contribute to the formation of new biological control strategies for insects.

Materials and methods

Insects, plant material and treatments

All experiments were conducted using healthy 3-year-old HJY and FDDB cultivar seedlings (20–25 cm in height). Tea plants were grown in approximately 2.0-L plastic pots containing acidic peat soil in a climate-controlled room (25 °C and 70% r.h., with an L14 : D10 photoperiod) and watered twice weekly. No pesticides were sprayed at any stage of plant growth.

E. onukii adults, with mixed age and sex and of unknown mating status, were collected from new shoots of tea plants via sweep nets at the Tea Experimental Plantation of Shandong Agricultural University in Tai'an, Shandong Province, China. The *E. onukii* were aspirated from the sweep nets after collection in the field and reared on the tea cultivar 'Longjing43' in ventilated cages (50 cm × 50 cm × 50 cm). The use of 'Longjing 43' tea seedlings for *E. onukii* feeding prior to experiments was to ensure consistent feeding conditions for the insects used in the experiment. A colony of *E. onukii* for use in the infestation experiments was established in laboratory. The cages were maintained in a climate-controlled chamber at 25 ± 2 °C and 70% ± 5% r. h., with a photoperiod of L14 : D10. The infestation experiments were performed in the climate-controlled chambers described above. Each three-year-old seedlings of HJY and FDDB cultivars were selected and placed in nylon mesh cages

(50 cm × 50 cm × 50 cm), and 100 adult *E. onukii* were introduced to each plant, respectively, as *E. onukii*-infested treatments for two tea cultivars. Uninfested HJY and FDDB tea seedlings not infested with *E. onukii* were used as experimental controls for respective cultivars. All treatments were replicated three times. After *E. onukii* continuous exposure 48 h, samples were taken from the tea seedling sapical leaf hazards, as material for subsequent protein preparation and lignin content determination.

Protein preparation and iTRAQ labeling

The iTRAQ analysis of this trial was performed at BGI (Shenzhen, China). Extraction of all proteins from *E. onukii* stressed under HJY and FDDB by phenol extraction method^[28]. There were three biological replicates due to each sample experiment. Protein concentrations were determined using the Bradford method to ensure the same amount of protein. Prepare 100 µg protein solution. Each sample was digested with 2.5 µg trypsin at a ratio of 1:40 (w : W) for 4 h. Different samples were recorded with different iTRAQ tag pairs at 37 °C.

LC-MS/MS analysis

Each sample was resoaked in buffer A (2% ACN and 0.1% FA in water) and centrifuged at 20,000 g for 10 min. Samples were put into the autosampler, and the supernatant was loaded onto a C18 trap column via an LC-20AD nano-HPLC instrument, with a speed of 5 µL/min for 8 min. The peptides were then eluted from the trapping column, based on which a column (75 µm id) packed inside the analytical C18 separation instrument was used. A speed increasing gradient of 300 nL/min from 8% to 35% buffer B (2% HO and 0.1% FA in ACN) was used over 35 min, then increased to 60% over 5 min, then held at 80% B for 5 min, finally decreased to 5% in 0.1 min, and stabilized for 10 min. Peptides were examined by ESI/NSI sources, followed by MS/MS data checking and analysis using Q ExactiveM Plus (Thermo Scientific) coupled online to UPLC. Whole peptides and ion fragments were detected by Orbitrap with resolution settings of 70,000 and 17,500, and NCE standard of 30. The electrospray voltage was 2.0 kV. Use automatic gain control (AGC) to prevent trap overcharging. The m/z amplitude of the MS scan was from 350 to 1,800. The standard for the initial mass fixation using MS was 100 m/z.

iTRAQ differential protein identification

The original MS/MS data were converted to MGF format using the ProteoWizard tool msConvert, and the database was used to search the exported MGF files. The search criteria were as follows: threshold offset in ion fraction cutoff was 0.05 (95% confidence); MS/MS fragment mass tolerance was ± 0.1 Da; enzyme specificity was set to trypsin; peptide tolerance was set to 0.05 Da; required for assays with at least one unique peptide to identify proteins. Proteins with a 1.2-fold change (average of all controls) and *p*-values (t-test of all controls) less than 0.05 were defined as differentially expressed proteins.

Lignin content and chromatic aberration determination

According to the methods above, HJY and FDDB samples infested with *E. onukii* and separate control treatments were collected. The lignin content determination was performed according to the lignin content kit instructions (CominbioR, Suzhou, China). The sample was dried at 80 °C until constant weight and pulverized, then passed through a 40 mesh sieve

and weighed about 5 mg (noted as W) in a 10 mL glass test tube. The test was divided into blank and assay tubes, 5 mg of sample, 1,000 μ L of reagent 1 and 40 μ L of perchloric acid were added to blank and assay tubes, respectively, sealed with a sealing film and mixed thoroughly, and then cooled naturally in a water bath at 80 °C for 40 min with shaking every 10 min. Then 1,000 μ L of reagent 2 was added to the test tubes, respectively. After thorough mixing, 40 μ L of supernatant was taken and 1,960 μ L of reagent 3 was added to the test tubes, respectively. One mL of the solution was taken in a quartz cuvette and the absorbance at 280 nm was measured as A. Lignin content was calculated according to the instructions of the lignin kit.

The color of different treatments was determined by a colorimeter (CM-5, KONICA MINOLTA, Japan), including three elements (L^* , a^* and b^*). L^* corresponds to luminance, with 0 value representing black and 100 representing white. a^* indicates redness/greenness, with '+' indicating red and '-' indicating green. b^* indicates yellow/blueness, with '+' indicating yellow and '-' indicating blue. Ten different sites (second leaf from the top) were selected as replicates for each treatment to measure the L^* , a^* and b^* values.

Insect feeding

Ten tea plants (HJY and FDDB) with similar growth, uniform leaf layers as well as no obvious pests and diseases, were selected as test seedlings, respectively. Four tea plants of each species were used as controls, then six tea plants were covered with insect-proof netting. In each species, half of the tea plants covered with insect-proof nets were accessed by 50–60 and half by 100–110 adult *E. onukii*, covered with transparent net bags to prevent escape. Samples were taken at 12, 24 and 48 h after feeding by *E. onukii*, respectively. Three biological replicates at each time point, a mixture of first and second leaves on new tea shoots were removed, frozen in liquid nitrogen, then brought back to the laboratory and stored at –80 °C for quantitative real-time polymerase chain reaction (qRT-PCR) for gene expression analysis.

Quantitative real-time polymerase chain reaction

Total RNA was extracted from the tea leaves by TRIZOL reagent (Invitrogen, Carlsbad, CA, USA). After extraction, 30 μ L of DEPC-treated water was prepared to dissolve the RNA. Then, 1% agarose gel electrophoresis was used to check the quality and purity of the total RNA, and a gel imaging system (GelDoc-1T2 315, BioSpectrum, USA) was used to observe the electrophoretic strip. First strand cDNA was synthesized using a reverse transcription kit (Thermo Fisher Scientific, Waltham, MA, USA) with oligo (dT)18 primers according to the manufacturer's instructions. A real-time PCR detection system (LightCycler 480 system, Roche Applied Science, Mannheim, Germany) was used as the fluorescence quantitative polymerase chain reaction instrument. The reaction system was compiled according to the SYBR@Green PCR Master Mix specifications (Takara, Bio Inc., Japan). The total reaction system for qRT-PCR was 20 μ L, including 0.4 μ L of forward primer, 0.4 μ L of reverse primer, 7.2 μ L of ddH₂O and 2 μ L of diluted cDNA (5 ng/ μ L). The PCR was performed under the following conditions: preliminary denaturation at 94 °C for 30 s, followed by 45 cycles of PCR at 95 °C for 5 s and annealing at 60 °C for 1 min, one cycle of melting curve generation at 72 °C for 5 s and 60 °C for 1 min, and final annealing at 50 °C for 30 s. The primers for qRT-PCR were shown in Supplemental Table S1. The cyclic threshold (Ct) was

considered the quantitative results, and the relative expression of each target gene in different samples was calculated by the following formula according to Livak and Schmittgen: $Ct = Ct_{target} - Ct_{control}$. Each gene was amplified with an internal reference. Each experiment was repeated in triplicate, and samples with no template and no reverse transcription were set up as two controls.

Bioinformatic analysis of the differentially expressed proteins (DEPs)

Blast v2.2.26 and Blast2 GO v4.5 were utilized to annotate biological processes, molecular functions, and cellular components of DEPs against the NCBI NR database and the latest Gene Ontology (GO) database (www.geneontology.org). We used the kyoto encyclopedia of genes and genomes (KEGG) database (www.genome.jp/kegg/pathway.html) in order to categorize the biochemical pathways involved and other types of molecular interactions. Cluster of Orthologous Groups of proteins (COG) databases were used for protein homology classification. COG functional classification of identified DEPs was performed in the STRING 9.0 database (<http://string-db.org>) using Blastx 2.2.24 + software (www.ncbi.nlm.nih.gov/COG).

Statistical analysis

The original files generated by the Q-Exactive system were analysed *via* Proteome Discoverer 1.4 software (Fisher Scientific Thermo, Waltham, MA, USA), and protein identification was performed *via* the Mascot search engine (Matrix Science, London, UK; version 2.3.02) against the UniProt Glycine max database. All statistical analyses were performed by using SPSS statistical software (version 19.0, SPSS Inc., Chicago, IL, USA). Statistically significant mean values were evaluated using two-way ANOVA with repeated measures analysis. Significant differences in changes in lignin content of two tea cultivars as well as tea plants under different densities of feeding by *E. onukii* treatments for all parameters were tested using Tukey's HSD test ($p < 0.05$).

Results

Protein identification analysis

The physiological condition of *E. onukii*-infested tea plants showed that the color of *E. onukii*-infested HJY leaves changed to light yellow with wrinkled and curled leaf periphery while compared to uninfested HJY. The internodes of the affected new shoots were shortened, and the shoots wilted in later stages. Compared with uninfested FDDB, the growth of damaged shoot tips of *E. onukii*-infested FDDB were stunted, and new shoots stopped developing. The leaf margins curled outward and the leaves lost luster (Fig. 1a). In our previous study, we found that *E. onukii* infestation affected the growth of both HJY and FDDB, reducing stem length, leaf area, leaf thickness and stem thickness. In addition, *E. onukii* infestation reduced the thickness of epidermal, fenestrated, spongy tissues on leaves, and pith diameter of thin-walled tissues between stem nodes. Meanwhile, *E. onukii* infestation reduced chlorophyll a and b and carotenoid content of HJY leaves, which further affecting photosynthetic rate^[6]. Chromatic aberration analysis of different treatments leaves showed that the leaves color of both two cultivars increased in lightness, as well as the leaves lighten in color and turn yellow after *E. onukii* infestation (Fig. 1b). Compared to the control, L^* values

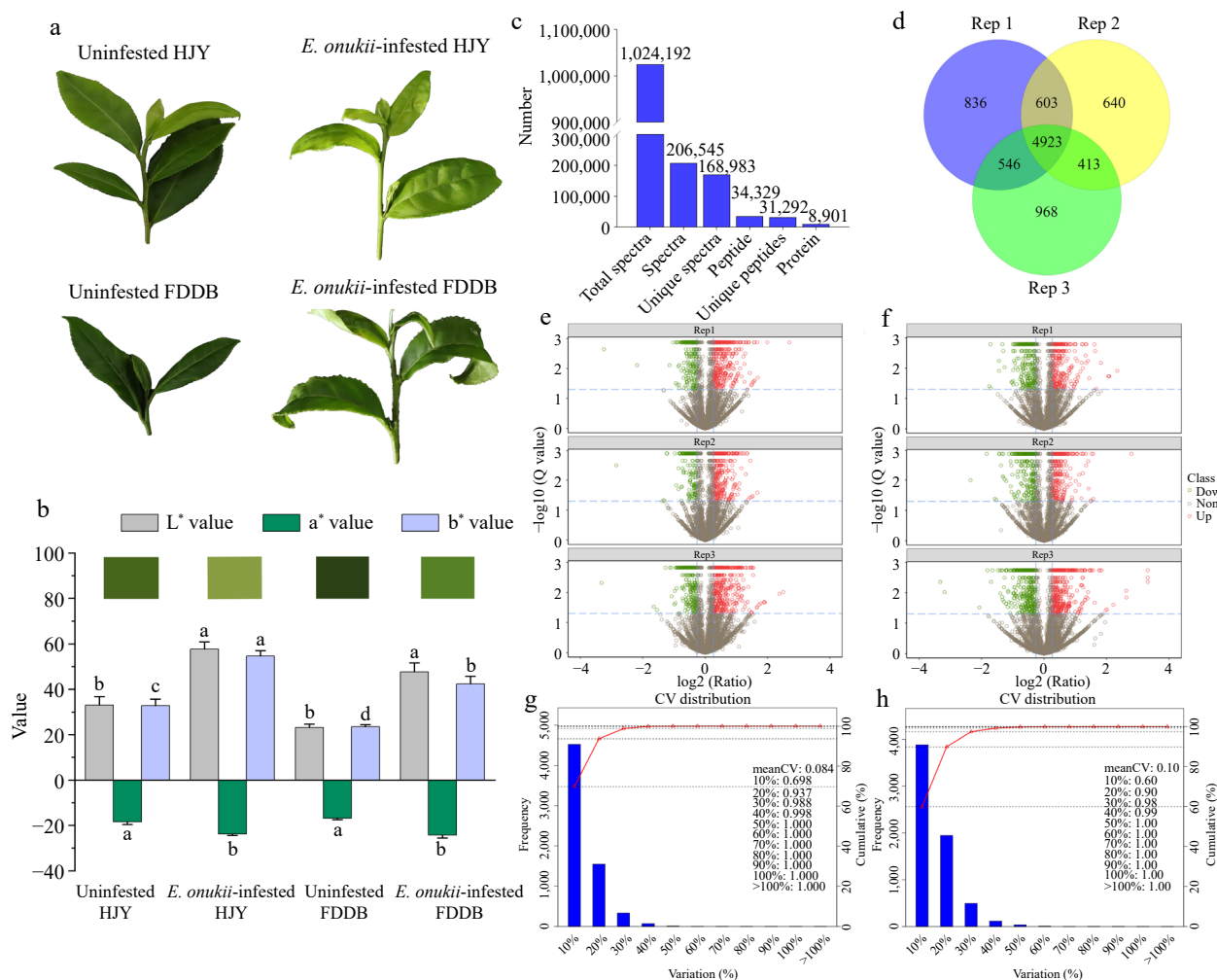


Fig. 1 Identification of DEPs in HJY and FDDB infested with *E. onukii*. (a) Physiological status of HJY and FDDB before and after *E. onukii*-infestation. (b) Chromatic aberration of HJY and FDDB leaves under uninfested and after *E. onukii*-infestation. Note: Different letters indicate significant differences between the different treatments (Tukey's HSD test, $p < 0.05$). (c) Total number of proteins identified by HJY and FDDB. (d) Number of proteins identified in three biological replicates. (e), (f) Volcano plots of significantly different proteins in three biological replicates in HJY and FDDB. Note: The X-axis of this plot was the protein difference folds (taken as \log_2) and the Y-axis was the corresponding $-\log_{10}$ (Q value). Q value < 0.05 and Fold change > 1.3 were the screening conditions for significantly different proteins. Red dots in the graph are up-regulated significantly proteins, green dots are down-regulated significantly proteins, and gray dots were proteins with no significant change. (g), (h) Coefficient of variation of protein analysis in HJY and FDDB.

increased by 74.3% in HJY, while the increase in FDDB was greater than HJY ($F = 21.845$; $df = 3$; $p < 0.01$). In addition, the a^* and b^* values of HJY increased by 29.3% and 66.8% respectively, while the FDDB parameter values increased by 42.9% and 80.4% respectively (a^* value: $F = 15.374$; $df = 3$; $p < 0.01$. b^* value: $F = 27.084$; $df = 3$; $p < 0.01$).

To investigate the resistance mechanism of tea plants against *E. onukii*, proteomic analysis of DEPs was performed via iTRAQ after feeding on FDDB and HJY by *E. onukii*. After mass spectrometry identification, a total of 168,983 specific spectra, 31,292 specific peptides and 8,901 proteins were identified in HJY and FDDB (Fig. 1c). Of the 8901 proteins identified, 6,485 proteins were identified in the two biological replicates, accounting for 72.86% of the total (Fig. 1d). The volcanoes of the proteins identified in HJY and FDDB in three biological replicates as shown Fig. 1e & f. Repeatability of quantification was assessed via coefficient of variation (CV), the CV of protein quantification in HJY was 0.084, it was 0.10 in FDDB. The

reproducibility of the quantitative analysis of proteins in this study was high, and the data analysis were accurate relatively (Fig. 1g & h).

Statistical and GO annotation analysis for DEPs

To further analyze the subcellular localization, molecular functions and biological processes of the DEPs, GO annotation analysis was performed on the DEPs. There were 331 and 245 up-regulated proteins in HJY and FDDB by the infestation of *E. onukii*, respectively, and 95 proteins were co-upregulated (Fig. 2a, Supplemental Table S2). There were 186 and 281 down-regulated proteins in HJY and FDDB under *E. onukii* stress, respectively, and 108 proteins were co-downregulated (Fig. 2b, Supplemental Table S2). The results showed that GO annotation analysis of DEPs was involved in 30 functional groups, including 10 biological processes, 10 cellular components and 10 molecular functions (Supplemental Table S3). The cellular component results showed that 95 up-regulated proteins were

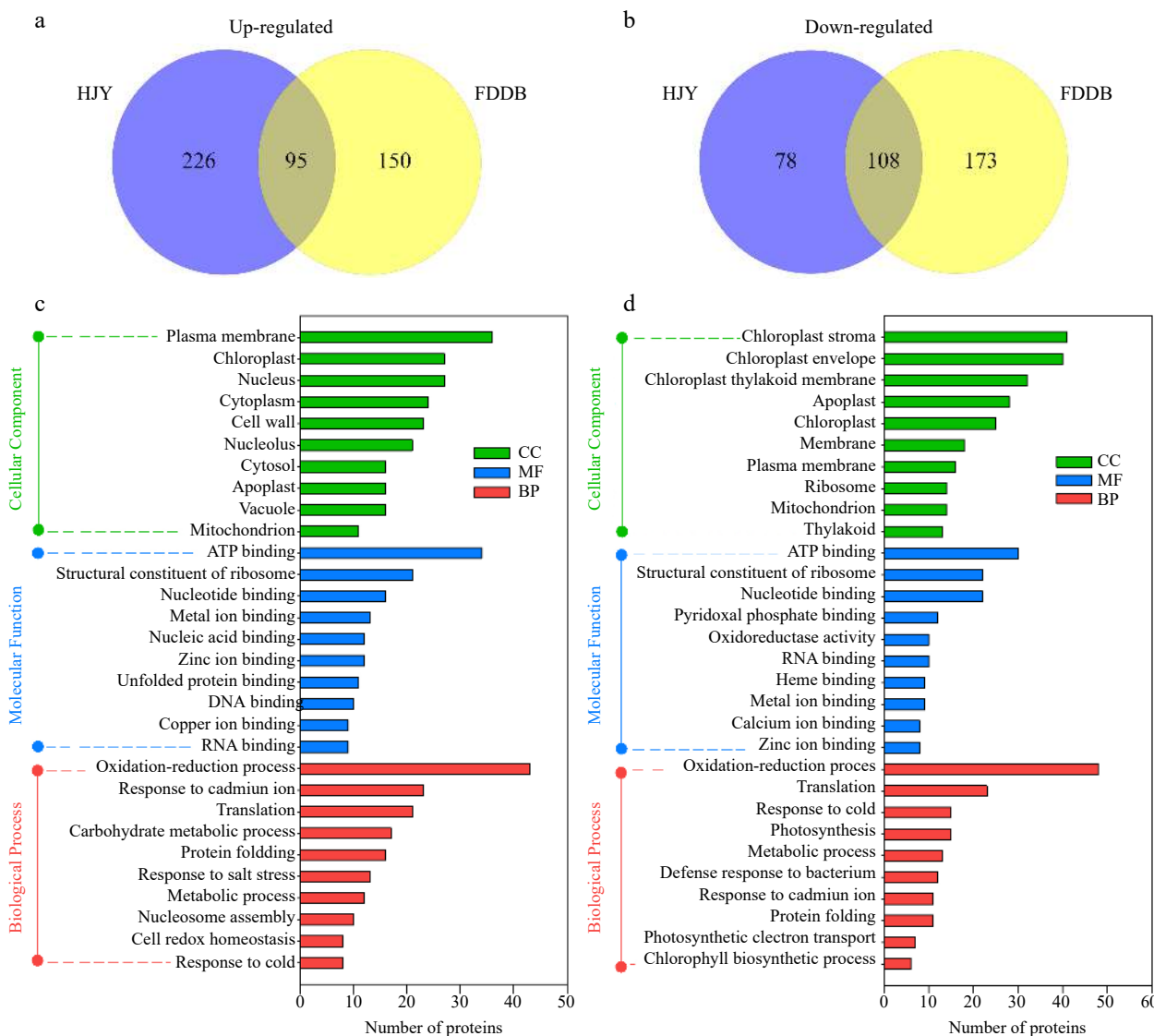


Fig. 2 GO annotation analysis of DEPs in HJY and FDDB infested with *E. onukii*. (a) Venn diagram of up-regulated significantly expressed proteins (1.3-fold) in HJY and FDDB. (b) Venn diagram of down-regulated significantly expressed proteins (0.77-fold) in HJY and FDDB. (c) GO analysis of 95 co-up-regulated proteins. (d) GO analysis of 108 co-down-regulated proteins.

mainly concentrated in 'plasma membrane', 'chloroplast' and 'nucleus'; the molecular function results showed these proteins were mostly in 'ATP binding', 'structural constituent of ribosome' and 'nucleotide binding'; the biological process results showed they were focused primarily on 'oxidation-reduction process' and 'response to cadmium ion' (Fig. 2c). The cellular component results showed that 108 down-regulated proteins were concentrated on the 'chloroplast stroma', 'chloroplast envelope' and 'chloroplast thylakoid membrane' in chief; the molecular function results showed they were largely centralized on 'ATP binding' and 'structural constituent of ribosome'; the biological process results showed they were centred on 'oxidation-reduction process' (Fig. 2d).

Clusters of COG analysis and KEGG enrichment analysis for DEPs

COG analysis and KEGG enrichment analysis were performed to further investigate the pathway and function of the DEPs. COG analysis showed that up-regulated and down-regulated

proteins, both in HJY and FDDB, were mainly concentrated in 'general function prediction only', 'posttranslational modification, protein turnover, chaperones', 'translation, ribosomal structure and biogenesis', 'carbohydrate transport and metabolism' and 'energy production and conversion' (Fig. 3a & b, Supplemental Table S4). DEPs were annotated into 23 COG categories, indicating that most DEPs encompass almost all aspects of the tea tree metabolism and growth. KEGG analysis showed that up-regulated DEPs (1.3-fold) were focused primarily on the pathway of 'metabolic pathways', 'biosynthesis of secondary metabolites', 'phenylpropanoid biosynthesis', 'biosynthesis of amino acids' and 'starch and sucrose metabolism'. DEPs were more numerous in 'carbon metabolism' and 'glycolysis/gluconeogenesis' in FDDB, whereas in 'ribosomal spliceosomes' of HJY (Fig. 3c, Supplemental Table S5). Down-regulated DEPs were concentrated in 'metabolic pathways', 'biosynthesis of secondary metabolites', 'carbon metabolism', 'glyoxylate and dicarboxylate metabolism' and 'carbon fixation in photosynthetic organisms' (Fig. 3d). In

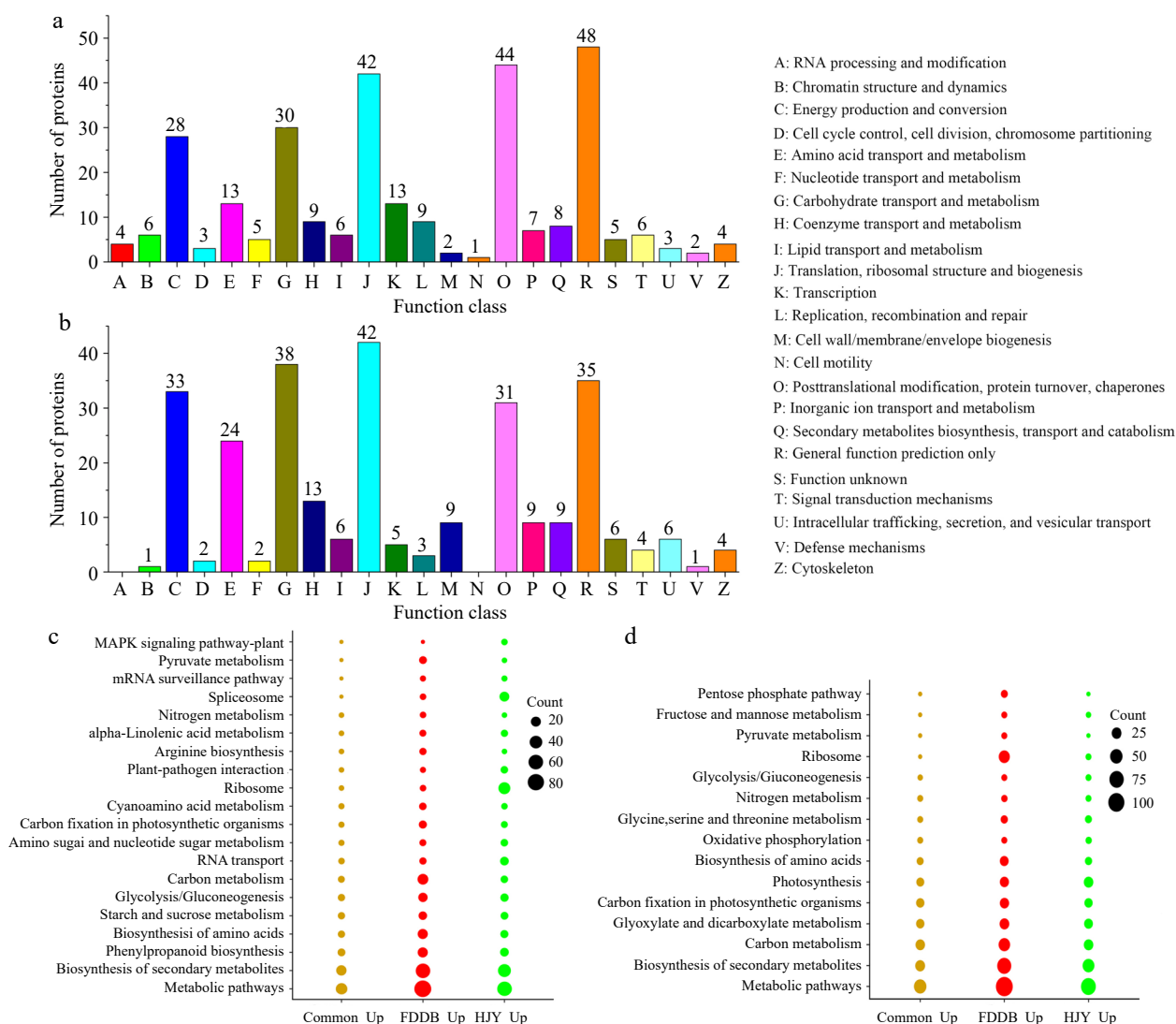


Fig. 3 COG analysis and KEGG enrichment analysis of DEPs in HJY and FDDB infested with *E. onukii*. (a) COG analysis of up-regulated significantly expressed proteins (1.3-fold). (b) COG analysis of down-regulated significantly expressed proteins (0.77-fold). (c) KEGG enrichment analysis of up-regulated significantly expressed proteins (1.3-fold). (d) KEGG enrichment analysis of down-regulated significantly expressed proteins (0.77-fold).

addition, DEPs of 'ribosome' were mostly up-regulated in HJY while they were down-regulated in FDDB.

Protein changes and enrichment pathways in tea plant after *E. onukii* infestation

In the Photosystem I (Ps I) pathway of photosynthesis, PsaF and LHCA1 in HJY were down-regulated after *E. onukii* infestation. In HJY and FDDB, PsbD1, PsbD2, PsbD3, PsbC1, PsbR, and PsbS2 in Photosystem II (Ps II) were co-downregulated after *E. onukii* infestation. Compared with the control, *E. onukii* infestation down-regulated PsbP1, PsbP2 and Psb27 in HJY, and significantly down-regulated PsbP3 in FDDB. In Cytochrome b6-f complex (Cyt b6/f), the expression of PetC in FDDB decreased by 0.63-fold, and there was no significant difference between HJY and the controls. In adenosine 5'-triphosphate (ATP) synthase, ATPb2, ATPβ2, ATPγ1, and ATPγ2 were down-regulated in HJY and FDDB after *E. onukii* infestation. ATPβ2 was down-regulated significantly in HJY, while ATPb1 and ATPδ were inhibited in FDDB. In photosynthetic electron transport, *E. onukii* infestation inhibited the expressions of FNR2 and FNR3

in HJY and FDDB. *E. onukii* infestation decreased the expressions of PC and FNR1 separately in HJY, as well as suppressed expression of FNR4 in FDDB (Fig. 4).

In the lignin biosynthetic pathway, POD1 was up-regulated 2.01-fold in HJY and 1.73-fold in FDDB after *E. onukii* infestation compared to the controls. POD6 was raised 1.31-fold in HJY after the feeding of *E. onukii*, whereas it was down 0.74-fold in FDDB. The express variety of CCR1 was induced in FDDB, and the expression amount was increased by 1.51-fold, but CCR2 was lowered by 0.77-fold. *E. onukii* infestation suppressed LAC1 in FDDB, and the expression of LAC1 was up-regulated by 5.49-fold (Fig. 5a).

Lignin content of two tea varieties before and after *E. onukii* infestation

To validate the proteomic results, the lignin content of two tea cultivars before and after *E. onukii* infestation were examined (Fig. 5b). The results showed that the lignin content of *E. onukii* -infested HJY was 333.45 ± 22.52 mg/g ($t = -12.44$; $df = 2.054$; $p = 0.006$), which was 6.5-fold higher than in lignin

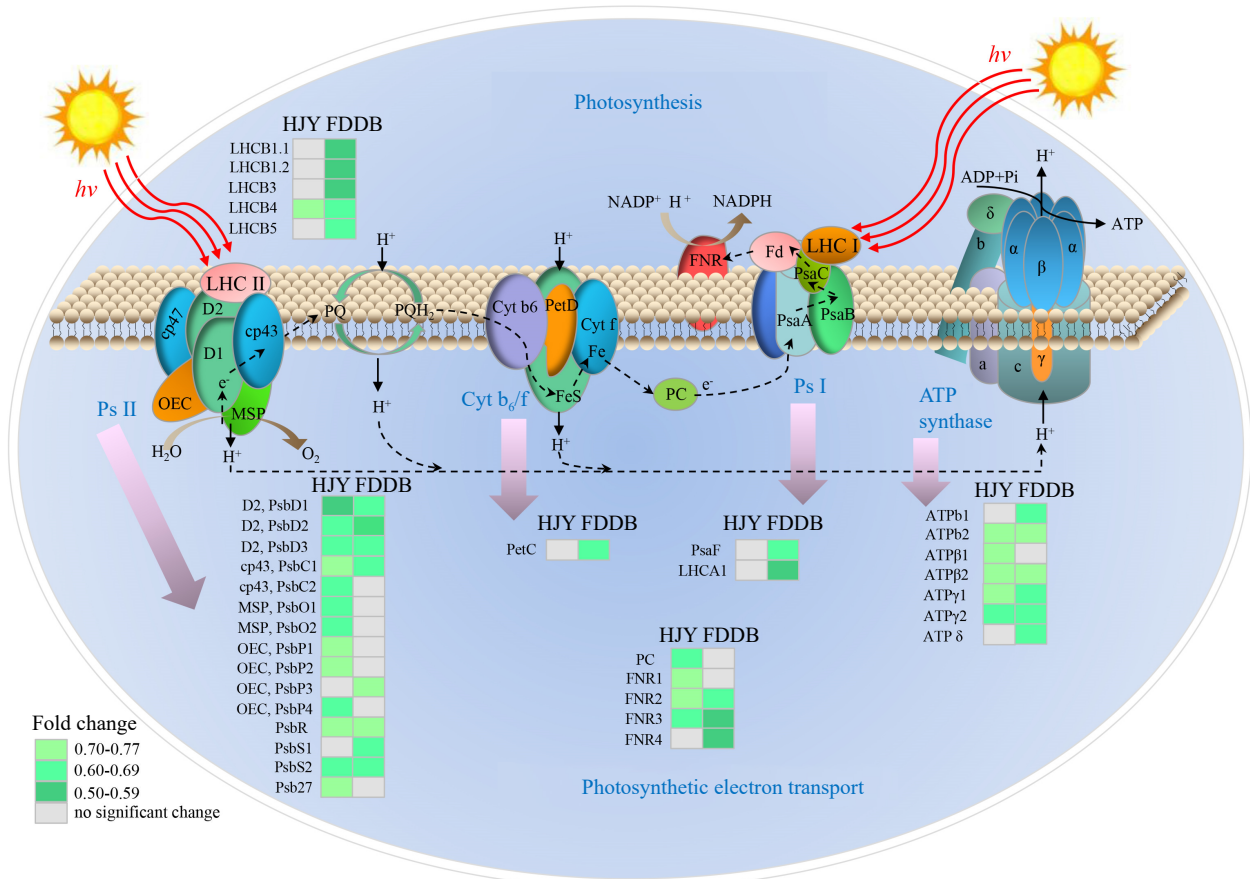


Fig. 4 Analysis of DEPs in the photosynthetic pathway of HJY and FDDB infested with *E. onukii*. Note: The multiplicative changes of DEP are presented in different colors, green represents down-regulation; gray represents no significant difference. LHC: Light harvesting complex; Psa: Photosynthetic apparatus; Psb: Photosynthetic bacteria; PC: Plastocyanin; FNR: Ferredoxin-NADP + Oxidoreductase; ATP: Adenosine 5'-triphosphate; Pet: Photoinduced electron transfer; Cyt b₆/f: Cytochrome b₆-f complex; Ps I: Photosystem I; Ps II: Photosystem II; OEC: Oxygen-evolving center; MSP: Manganese stabilizing protein; PQ: Plastoquinone; ADP: Adenosine-diphosphate; NADPH: Nicotinamide adenine dinucleotide phosphate. The serial numbers of the protein names in the figure are shown in Supplemental Table S6.

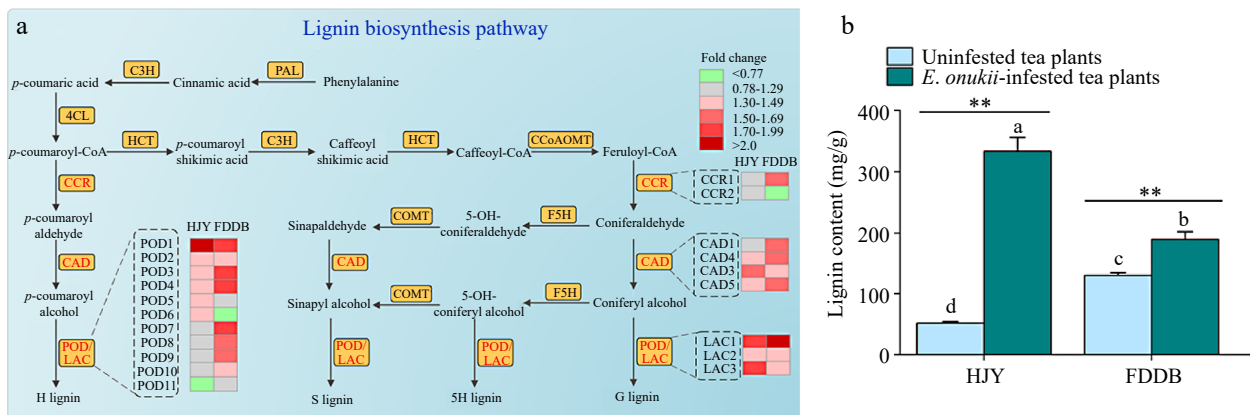


Fig. 5 Effect of *E. onukii* infestation on lignin synthesis in HJY and FDDB. (a) Analysis of DEPs in the lignin biosynthesis pathway of HJY and FDDB infested with *E. onukii*. Note: The multiplicative changes of DEPs were presented in different colors, green indicated down-regulated DEPs; red indicated up-regulated DEPs; and gray indicated proteins with no significant difference. POD: Peroxidase; CCR: Cinnamoyl-CoA reductase; CAD: Cinnamyl-alcohol dehydrogenase; LAC: Laccase; HCT: Hydroxycinnamoyl transferase; C3H: Coumaric acid 3-Hydroxylase; C4H: Cinnamic acid-4-hydroxylase; COMT: Catechol O-methyltransferase; F5H: Ferulate 5-hydroxylase; CCoAOMT: Caffeoyl-CoA 3-O-methyltransferase; G lignin: guaiacyl-type lignin; 5H lignin: 5-Hydroxy-guaiacyl lignin; S lignin: Syringyl monolignol lignin; H lignin: p-hydroxyphenyl lignin. The serial numbers of the protein names in the figure are shown in Supplemental Table S6. (b) Lignin content of two tea cultivars before and after *E. onukii* infestation. Note: Different letters indicate significant differences between the different treatments (Tukey's HSD test, p < 0.05). Asterisks designate a significant difference between control and *E. onukii*-infested plants of the same cultivar (independent samples t-test, p < 0.01).

content of uninfested HJY leaves. Compared to the control, there was a significant difference in the lignin content of *E. onukii*-infested HJY ($p < 0.01$). The lignin content of FDDB was less variable compared to the variation in HJY, and *E. onukii*-infested FDDB lignin content was 189.79 ± 12.06 mg/g ($t = -4.727$; $df = 4$; $P = 0.009$), which was 1.5-fold higher than in lignin content of uninfested FDDB. Compared with the control, lignin content of FDDB were not obviously affected by the *E. onukii* infestation ($p < 0.05$).

Analysis of gene expression in tea plants infested with *E. onukii*

To confirm the validity of the iTRAQ data, qRT-PCR was used to monitor the expression pattern of the corresponding genes encoding the differential proteins in tea plants infested with 50 and 100 *E. onukii* (Fig. 6, Supplemental Table S7). In the 50 *E. onukii*-infested treatment, the expression level of *CsLAC2* was 131.00-fold of the controls at 12 h, followed by a sharp decrease. The expression level of *CsLAC3* increased gradually after the feeding of *E. onukii*, reaching 35.02-fold at 24 h. The expression level of *CsCCRs* showed a trend of increasing, then decreasing and then re-increasing with time after the *E. onukii* feeding. The expression level of *CsCCR1* reached 426.01-fold at 12 h, then dropped sharply to 11.17-fold at 24 h, and increased again to 181.24-fold at 48 h. The expression level of *CsPOD1* reached the max at 12 h after *E. onukii* feeding, which was 18.70-fold of the controls, then it decreased to 4.60-fold at 24 h, finally it slightly increased to 6.86-fold at 48 h. The expression of *CsPOD2* reached the max at 24 h, which was 58.32-fold of the controls, and it was significantly higher than the expression level at other moments. The trend of transcript expression level of the *CsCADs* over time was similar to *CsCCRs*, the expression level of *CsCAD3* rose to 157.52-fold at 12 h, then dropped sharply to 18.88-fold at 24 h, and rose again to 345.37-fold at 48 h. The expression level of *CsCAD5* reached a maximum at 48 h with 456.35-fold that of the controls, followed by a higher level at 12 h, but there was no significant difference in the expression level between 0, 12 and 24 h.

In the 100 *E. onukii*-infested treatment, the expression level of *CsLAC1* reached a maximum of 351.50-fold of the controls at 12 h, then it decreased to 23.83-fold at 24 h, and it increased slightly to 57.53-fold at 48 h. The expression level of *CsLAC2* was 150.89-fold and 168.06-fold higher at 12 and 48 h, respectively. The expression levels of *CsCCR1* and *CsCCR2* were reached a maximum at 48 h, with 26.10-fold and 183.91-fold of the controls, respectively. There were no significant difference in the expressions of *CsCCR1*, *CsCCR2* and the controls at 12 and 24 h. The expression level of *CsPOD2* was 6.20-fold at 48 h, and showed a gradual increase trend over the 48 h. The expression level of *CsCAD5* reached 514.62-fold of the control at 12 h, then it dropped sharply to 8.63-fold at 24 h, and it rose again to 100.39-fold at 48 h.

Discussion

In our study, compared to uninfested tea plants, the *E. onukii*-infested HJY leaf color turned light yellow, as well as the leaves circumference were wrinkled and curled. The affected new shoots internodes were shortened, and the shoots and leaves become wilted in the later stages. This phenomenon correlates with *E. onukii* infestation reducing HJY leaves chlorophyll a, b and carotenoid contents, which further reduced photosynthetic rate thereby affecting the tea plants normal growth and

development. In addition, *E. onukii* infestation altered free amino acids, tea polyphenols, caffeine and catechins content in HJY, which also affected the tea plant quality development^[16]. Compared with uninfested tea plants, the damaged bud tips growth were hindered in *E. onukii*-infested FDDB, and the new buds stopped developing. Curling of the leaf margins occurred outward and the leaves color turned yellow and lost luster, indicating that stinging pest infestation affects host plants growth traits and developmental status^[28,29]. Our previous study also revealed that *E. onukii* infestation affected the HJY and FDDB growth, it mainly reduces tea plants stem length, leaf area, leaf thickness and stem thickness^[16].

A total of 168,983 specific spectra, 31,292 specific peptides and 8,901 proteins were identified in HJY and FDDB after feeding by *E. onukii*. There were 331 and 245 up-regulated proteins, respectively, and 95 proteins co-regulated in HJY and FDDB after *E. onukii* infestation. Meanwhile, there were 186 and 281 down-regulated proteins, respectively, and 108 co-regulated proteins in two tea plant cultivars. After feeding by *E. onukii*, the number of up-regulated proteins in HJY was more than that of in FDDB, while the number of down-regulated proteins was less than that of in FDDB. We hypothesized that there was the difference in the resistant of two tea cultivars to *E. onukii*. Efficient protein extraction methods could improve accuracy of experimental results, DC-EPG tests showed that *E. onukii* had different feeding tendencies on different tea plants cultivars^[30,31]. Different tea plant cultivars may use different defense strategies to cope with insects, and the highly sensitive tea cultivars would activate more defense proteins to resist pest stress^[32].

In our study, GO annotation analysis, COG enrichment and KEGG pathway analysis were performed in order to further analyze the functions of DEPs. GO annotation analysis showed that DEPs were focused on 'plasma membrane', 'ATP binding', and 'oxidation-reduction process', which was similar to the phenomena observed after the infestation of pepper *Capsicum annuum* L. by *Bemisia tabaci*^[33]. COG enrichment showed that DEPs were concentrated on 'translation, ribosomal structure and biogenesis' and 'general function prediction only', and these DEPs may be associated with the resistance of tea plant to *E. onukii*. The sustainability of resistance depends on the interactions of DEPs and the way in which they accumulate or activate plant defenses^[34,35]. DEPs of 'ribosome' in HJY were mostly up-regulated compared with FDDB. It is speculated that HJY may be more sensitive to *E. onukii* than FDDB. Six ribosomal proteins showed that higher abundance in the high levels of resistance-control treatments than in the high levels of susceptibility-control treatments when peppers were infested by *B. tabaci*^[33]. The role of 'ribosome' in plant insect resistance needs further investigation. KEGG enrichment pathway analysis showed that the DEPs were centered on 'metabolic pathways' and 'biosynthesis of secondary metabolites', and the results were similar to the study^[36]. Our results indicated that most DEPs encompass the broad aspects of the tea plant metabolism and growth, hypothesizing that they may be involved in the defense and compensation mechanisms in two tea cultivars against *E. onukii* infestation.

In photosynthetic electron transport, the expressions of FNR2 and FNR3 were inhibited in both HJY and FDDB, and relevant proteins involved in photosynthesis showed down-regulation in response to the *E. onukii* infestation. For example, some

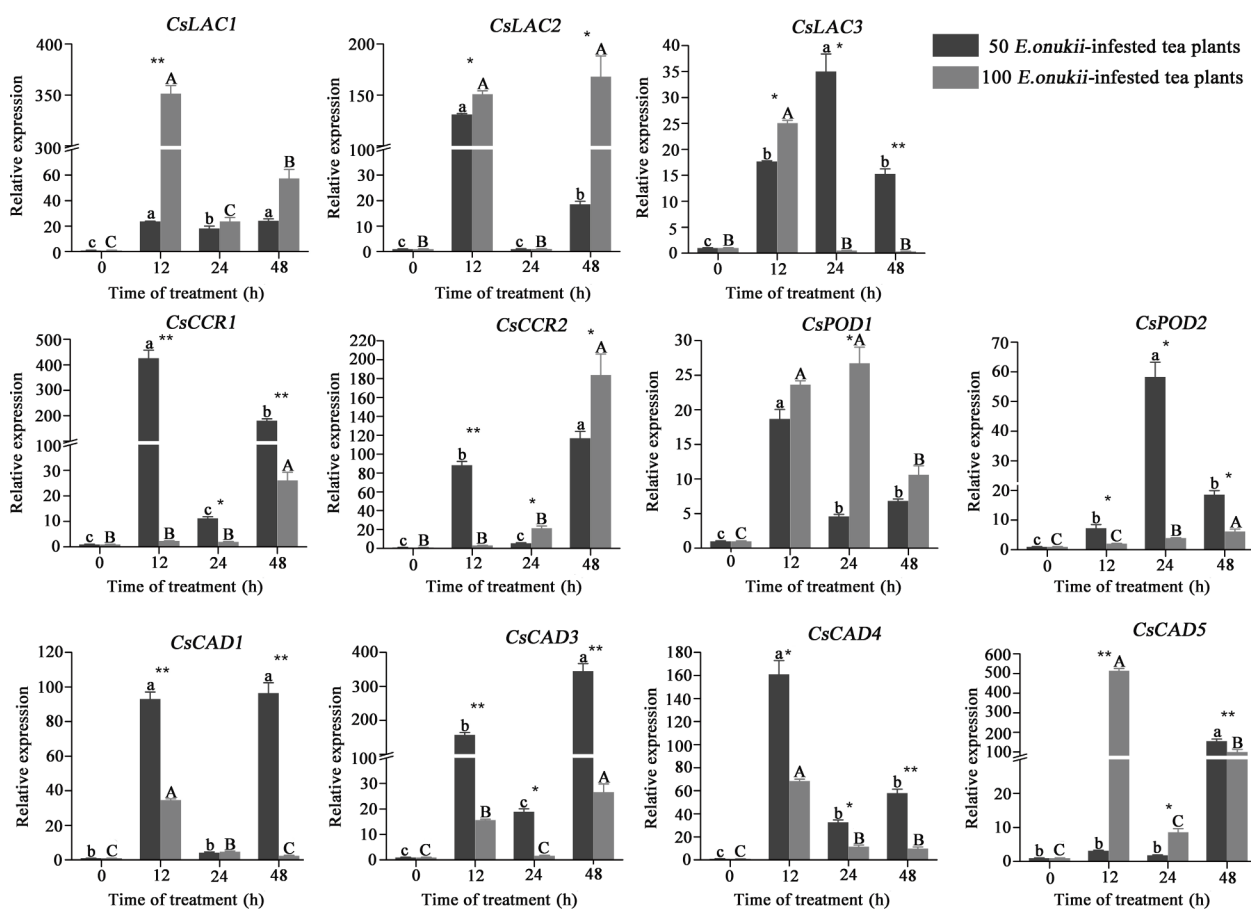


Fig. 6 Expression of differential protein-coding genes in tea plants infested by *E. onukii* at two different densities. Note: Different lowercase letters indicate the differences between diverse times under 50 *E. onukii*-infested treatment, and different capital letters indicate the differences between diverse times under 100 *E. onukii*-infested treatment. Asterisk indicates a significant group difference on expression levels of genes at different densities, * indicates $p \leq 0.05$, ** indicates $p \leq 0.01$. Transcriptional expression level of differential protein-coding genes in tea plants after *E. onukii* feeding, and sampling time was 0, 12, 24 and 48 h. Light gray represents the tea plants fed by 100 *E. onukii*, as the high-density *E. onukii*-infested tea plant treatments; dark gray represents the tea plants fed by 50 *E. onukii*, as the low-density *E. onukii*-infested tea plant treatments.

sugarcane cultivars exhibit down-regulation of defense protein genes involved in photosynthesis and energy metabolism pathways when subjected to the infestation of *Diatraea saccharalis*[37]. Some Psbs, such as PsbD1, PsbD2, PsbD3, PsbC1, PsbR and PsbS2, in Ps II of two tested tea plant cultivars were all co-downregulated. When tomato plants were fed by potato aphid *Macrosiphum euphorbiae*, genes associated with photosynthesis were generally down-regulated throughout the infestation period, but the number of differentially expressed genes was greater after 48 h[38]. Down-regulation of photosynthesis-related genes is a protective response to biotic stress, which could reduce the turnover rate of many photosynthetic proteins, thus allowing plants to devote resources to their immediate defense needs[37,39]. Insect attack can promote photosynthesis of plants[40]. A higher proportion of proteins increased in peppers after infestation by *B. tabaci*, indicating photosynthesis-related proteins were involved in the defense process of peppers against *B. tabaci*[33]. Increased photosynthetic activity could supplement the leaf area damage caused by insects[41].

The woody tissues of plant leaves and stems are often damaged by piercing sucking insects, which activate proteins

associated with the lignin synthesis pathway involved in the response of plants to biotic stress[42,43]. We found that a series of lignin-synthesizing proteins, including PAL, C4H, 4CL, C3H, F5H, and COMT, were activated and functioned after *E. onukii* infestation in two tea cultivars. Biotic stresses induce the lignification of cell walls and increase the flavonoid level in plants[44]. In *Pyrus bretschneideri*, PbrMYB169 TF could activate the promoters of lignin biosynthesis genes such as LAC18, HCT2, C3H1, CCOMT2, CCR1, 4CL1, 4CL2 and CAD by binding to the AC element in the promoters of them, thereby increasing the deposition of lignin in the kernel cells[45]. TFs EjMYB8 and EjERF39 synergistically transactivate the Ej4CL1 promoter and regulate lignin biosynthesis in loquat fruit[46]. He et al. found OsPAL8 could mediate resistance to rice against *Nilaparvata lugens* by regulating lignin biosynthesis and accumulation[47]. Overexpression of CmMYB15 and CmMYB19 TF genes in *Chrysanthemum morifolium* limits aphid invasion by activating lignin biosynthesis genes and accumulating lignin[48,49]. In *Malus domestica*, MdMYB46 could increase secondary cell wall biosynthesis and lignin deposition by binding to lignin biosynthesis-related genes, such as CCR, COMT and CAD[50]. We hypothesized that lignin synthesis pathway-related proteins are critical for the resistance of tea plants to *E. onukii*.

In lignin biosynthesis pathway, most PODs were up-regulated significantly under *E. onukii*-stress, hypothesizing PODs may be involved in the process of tea plant resistance to biotic stresses^[51]. In the plant growth and development process, PODs are involved in lignin biosynthesis, as well as cell wall loosening and hardening^[52,53]. In *Sitophilus zeamais* and *Prostephanus truncatus*, the activities of soluble endosperm PODs were 1.38- and 0.85-fold higher than that of the control after 48 h of infestation with insects, respectively^[54]. In addition, there was an interaction between soluble endosperm POD and resistance of maize to the corn pest *Sitophilus zeamais*^[55]. There was a tendency for LACs to be up-regulated in plants subjected to biotic stress. For example, LACs could participate in physiological processes, such as plant secondary cell wall development and catalyzing the lignin monomer polymerization, which in turn enhance cotton's tolerance to *Heterodera glycines* Ichinohe, *Helicoverpa armigera* Hübner and *Aphis gossypii* Glover^[56,57]. Our results showed that LACs including LAC1, LAC2, and LAC3 were significantly up-regulated in HJY and FDDB after infestation by *E. onukii*.

In our study, the expression levels of *CsCAD1*, *CsCAD3*, and *CsCAD4* increased sharply within 12 h in the low density of *E. onukii*-infested treatment, and *CsCAD5* increased sharply in the high density of *E. onukii*-infested treatment, speculating that CAD may be involved in the insect resistance of tea plants. CAD is dependent on NADPH for the reduction of cinnamaldehyde and its derivatives, which is the last pivotal enzyme step in catalyzing the biosynthetic pathway of lignin monomers^[58]. The total lignin content of most plants decreases, when CAD activity is reduced or inhibited^[59]. The expression levels of two LAC genes, including *CsLAC2* and *CsLAC2*, appeared the trend of first increasing, secondly decreasing, and then increasing sharply. Many differential genes in resistant and susceptible tea cultivars exhibited an upward and then downward trend in response to *E. onukii* feeding. There may be a process of 'stress response – adaptation – defense response' in tea plants^[60]. The early stage after *E. onukii* infestation is the 'stress response process' of the tea plants to cope with the pest stimulation, followed by gradual adaptation and entering the process of the 'defense response', and the genes expression would show a phenomenon of increasing then decreasing then increasing again, this phenomenon was also found in the previous study by Qiao et al.^[20] Many differentially expressed genes in both resistant and sensitive tea plant cultivars showed an increasing and then decreasing trend after 0, 12 and 24 h of pests feeding^[60], these results suggest that this is a generalized process which tea plants respond to pest infestation. Five *CsLACs* were up-regulated in tea plants attacked by pierce-sucking or/and chewing insect pests, indicating their potential functions in tea resistance against herbivorous pests^[14]. Simulating the expression pattern of *CsLACs* in tea plants under the attack of *Ectropis obliqua*, nine genes were expressed at the highest level at 6 h, 18 genes were expressed at the highest level at 12 h, and seven genes were expressed at the higher level at 24 h, suggesting *CsLACs* have different expression pathways^[61]. Overexpression of *GhLac1* in the cotton genus enhances a broad-spectrum biodefense response against pests through increasing lignin deposition in *Gossypium hirsutum*^[56]. Therefore, we hypothesized that *CsLACs* play a critical role in the response of tea plants to *E. onukii*. In addition, some genes

such as *CsLAC3*, *CsCCR1*, *CsPOD2*, *CsCAD1*, *CsCAD2* and *CsCAD4*, were significantly higher in the low-density *E. onukii* feeding than in the high-density *E. onukii* feeding, suggests that the plant defense responses activation was closely related to plant cultivars, infestation time and insect density^[62]. Feeding damage degree and phytophagous insects density are important factors influencing plant system-induced responses and insect interactions^[63].

Conclusions

The focus of this study was to identify the differences associated with defense mechanisms that may be involved in the tolerance of tea plants to *E. onukii* through examining changes in DEPs. In summary, the study analyzed the DEPs of two tea plant cultivars HJY and FDDB in response to *E. onukii* infestation. There were 168,983 specific spectra, 31,292 specific peptides, and 8,901 proteins identified in HJY and FDDB after *E. onukii* infestation. Proteins involved in physiological processes, such as plant stress defense, photosynthesis, carbohydrate utilization, and protein degradation, were affected in the injured tea plants after *E. onukii* feeding. Most of the proteins involved in photosynthesis, such as PHCs, FNRs, PSBs and LHCs, showed down-regulation when tea plants were subjected to infestation by *E. onukii*. Many proteins involved in lignin biosynthesis, such as PODs, CADs, and LACs, were upregulated in response to infestation by *E. onukii*. The qRT-PCR results showed that the expression levels of 11 protein-coding genes changed significantly in tea plants after infestation by *E. onukii*. As the feeding time of *E. onukii* progressed, the expression level of the lignin synthesis related genes, including *CsLAC1*, *CsLAC2*, *CsCCR1*, *CsCAD1*, *CsCAD3*, and *CsCAD4*, showed a trend of increasing at the beginning, and then dramatically decreasing, followed by increasing. We speculate that there may be a process of 'stress response-adaptation-defense response' in tea plants against *E. onukii* infestation.

Author contributions

The authors confirm contribution to the paper as follows: study conception and design: Tian Y, Lun X; data collection: Cao Y, Zhang X; analysis and interpretation of results: Jin M, Guan F, Wang L; draft manuscript preparation: Zhang R, Zhao Y, Zhang Z. All authors reviewed the results and approved the final version of the manuscript.

Data availability

The raw data supporting the conclusions of this article will be made available by the authors, without undue reservation. All data generated or analysed during this study are included in supplementary information files.

Acknowledgments

We acknowledge financial support from Key Research and Development Program of Shandong Province (2022LZGCQY020), National Natural Science Foundation of China (31501651; 32302612), Natural Science Foundation of Shandong Province (ZR2020MC122; ZR2020QC055) and Daizong Top Talent Cultivation Project in Industry of Tai'an.

Conflict of interest

The authors declare that they have no conflict of interest.

Supplementary Information accompanies this paper at (<https://www.maxapress.com/article/doi/10.48130/bpr-0023-0039>)

Dates

Received 10 October 2023; Revised 29 November 2023; Accepted 4 December 2023; Published online 1 February 2024

References

- dos Santos TB, Budzinski IGF, Marur CJ, Petkowicz CLO, Pereira LFP, et al. 2011. Expression of three galactinol synthase isoforms in *Coffea arabica* L. and accumulation of raffinose and stachyose in response to abiotic stresses. *Plant Physiology and Biochemistry* 49(4):441–48
- Jeyaraj A, Liu S, Zhang X, Zhang R, Shangguan M, et al. 2017. Genome-wide identification of microRNAs responsive to *Ectropis oblique* feeding in tea plant (*Camellia sinensis* L.). *Scientific Reports* 7:13634
- Fuchs B, Krauss J. 2019. Can *Epichloë* endophytes enhance direct and indirect plant defence? *Fungal Ecology* 38:98–103
- Mottiar Y, Vanholme R, Boerjan W, Ralph J, Mansfield SD. 2016. Designer lignins: harnessing the plasticity of lignification. *Current Opinion in Biotechnology* 37:190–200
- Li L, Hao R, Yang X, Feng Y, Bi Z. 2023. *Piriformospora indica* increases resistance to *Fusarium pseudograminearum* in wheat by inducing phenylpropanoid pathway. *International Journal of Molecular Sciences* 24:8797
- Miao YC, Liu CJ. 2010. ATP-binding cassette-like transporters are involved in the transport of lignin precursors across plasma and vacuolar membranes. *Proceedings of the National Academy of Sciences of the United States of America* 107:22728–33
- del Río JC, Rencoret J, Gutiérrez A, Lan W, Kim H, et al. 2021. Lignin monomers derived from the flavonoid and hydroxystilbene biosynthetic pathways. In *Recent advances in polyphenol research*, eds. Reed JD, de Freitas VAP, Quideau S. Vol. 7. UK: John Wiley & Sons. pp. 177–206. <https://doi.org/10.1002/9781119545958.ch7>
- del Río JC, Rencoret J, Gutiérrez A, Elder T, Kim H, et al. 2020. Lignin monomers from beyond the canonical monolignol biosynthetic pathway: another brick in the wall. *ACS Sustainable Chemistry & Engineering* 8:4997–5012
- Liu N, Wang Y, Li K, Li C, Liu B, et al. 2023. Transcriptional analysis of tea plants (*Camellia sinensis*) in response to salicylic acid treatment. *Journal of Agricultural and Food Chemistry* 71:2377–89
- Cheng S, Yan J, Meng X, Zhang W, Liao Y, et al. 2018. Characterization and expression patterns of a cinnamate-4-hydroxylase gene involved in lignin biosynthesis and in response to various stresses and hormonal treatments in *Ginkgo biloba*. *Acta physiologiae plantarum* 40:7
- Ponniah SK, Shang Z, Akbudak MA, Srivastava V, Manoharan M. 2017. Down-regulation of hydroxycinnamoyl CoA: shikimate hydroxycinnamoyl transferase, cinnamoyl CoA reductase, and cinnamyl alcohol dehydrogenase leads to lignin reduction in rice (*Oryza sativa* L. ssp. japonica cv. Nipponbare). *Plant Biotechnology Reports* 11:17–27
- Liu W, Jin Y, Li M, Dong L, Guo D, et al. 2018. Analysis of CmCADs and three lignifying enzymes in oriental melon ('CaiHong7') seedlings in response to three abiotic stresses. *Scientia Horticulturae* 237:257–68
- Berthet S, Demont-Caulet N, Pollet B, Bidzinski P, Cézard L, et al. 2011. Disruption of *LACCASE4* and 17 results in tissue-specific alterations to lignification of *Arabidopsis thaliana* stems. *The Plant Cell* 23:1124–37
- Yu Y, Xing Y, Liu F, Zhang X, Li X, et al. 2021. The laccase gene family mediate multi-perspective trade-offs during tea plant (*Camellia sinensis*) development and defense processes. *International Journal of Molecular Sciences* 22:12554
- Wang YN, Tang L, Hou Y, Wang P, Yang H, et al. 2016. Differential transcriptome analysis of leaves of tea plant (*Camellia sinensis*) provides comprehensive insights into the defense responses to *Ectropis oblique* attack using RNA-Seq. *Functional & Integrative Genomics* 16:383–98
- Tian Y, Zhao Y, Zhang L, Mu W, Zhang Z. 2018. Morphological, physiological, and biochemical responses of two tea cultivars to *Empoasca onukii* (Hemiptera: Cicadellidae) infestation. *Journal of economic entomology* 111:899–908
- Wang Z, Huang R, Moon DG, Ercisli S, Chen L. 2023. Achievements and prospects of QTL mapping and beneficial genes and alleles mining for important quality and agronomic traits in tea plant (*Camellia sinensis*). *Beverage Plant Research* 3:22
- Zhang X, Liu L, Luo S, Ye X, Wen W. 2023. Research advances in aluminum tolerance and accumulation in tea plant (*Camellia sinensis*). *Beverage Plant Research* 3:18
- Zhou Y, Liu Y, Wang S, Shi C, Zhang R, et al. 2017. Molecular cloning and characterization of galactinol synthases in *Camellia sinensis* with different responses to biotic and abiotic stressors. *Journal of Agricultural and Food Chemistry* 65:2751–59
- Qiao D, Yang C, Guo Y, Chen J, Chen Z. 2023. Transcriptome and co-expression network analysis uncover the key genes mediated by endogenous defense hormones in tea plant in response to the infestation of *Empoasca onukii* Matsuda. *Beverage Plant Research* 3:4
- Zhang Z, Luo Z, Gao Y, Bian L, Sun X, et al. 2014. Volatiles from non-host aromatic plants repel tea green leafhopper *Empoasca vitis*. *Entomologia Experimentalis et Applicata* 153:156–69
- Zhang Z, Zhou C, Xu Y, Huang X, Zhang L, et al. 2017. Effects of intercropping tea with aromatic plants on population dynamics of arthropods in Chinese tea plantations. *Journal of Pest Science* 90:227–37
- Jin S, Chen ZM, Backus EA, Sun XL, Xiao B. 2012. Characterization of EPG waveforms for the tea green leafhopper, *Empoasca vitis* Göthe (Hemiptera: Cicadellidae), on tea plants and their correlation with stylet activities. *Journal of Insect Physiology* 58:1235–44
- Wu LJ, Li F, Song Y, Zhang ZF, Fan YL, et al. 2023. Proteome analysis of male accessory gland secretions in the diamondback moth, *Plutella xylostella* (Lepidoptera: Plutellidae). *Insects* 4:132
- Rahul K, Makwana P, Ghosh S, Pappachan A. 2023. Why Biotechnology Needed in Insects?. In *Introduction to Insect Biotechnology*, eds. Kumar D, Shukla S. Netherlands: Springer, Cham. pp. 17–44. https://doi.org/10.1007/978-3-031-26776-5_2
- Zhang J, Zhang L, Qiu J, Nian H. 2015. Isobaric tags for relative and absolute quantitation (iTRAQ)-based proteomic analysis of *Cryptococcus humicola* response to aluminum stress. *Journal of Bioscience and Bioengineering* 120:359–63
- Sun XY, Liu QH, Huang J. 2018. iTRAQ-based quantitative proteomic analysis of differentially expressed proteins in *Litopenaeus vannamei* in response to infection with WSSV strains varying in virulence. *Letters in applied microbiology* 67:113–22
- McAuslane HJ, Chen J, Carle RB, Schmalstig J. 2004. Influence of *Bemisia argentifolii* (Homoptera: Aleyrodidae) infestation and squash silverleaf disorder on zucchini seedling growth. *Journal of economic entomology* 97(3):1096–105
- Li Q, Tan W, Xue M, Zhao H, Wang C. 2013. Dynamic changes in photosynthesis and chlorophyll fluorescence in *Nicotiana tabacum* infested by *Bemisia tabaci* (Middle East-Asia Minor 1) nymphs. *Arthropod-Plant Interactions* 7:431–43
- Wang W, Vignani R, Scali M, Cresti M. 2006. A universal and rapid protocol for protein extraction from recalcitrant plant tissues for proteomic analysis. *Electrophoresis* 27:2782–86
- Miao J, Han B. 2007. Probing behavior of the tea green leafhopper on different tea plant cultivars. *Acta Ecologica Sinica* 27:3973–82

32. Chen ZM, Sun XL, Dong WX. 2012. Genetics and chemistry of the resistance of tea plant to pests. In *Global tea breeding: Achievements, challenges and perspectives*. Berlin, Heidelberg: Springer. pp. 343–60. https://doi.org/10.1007/978-3-642-31878-8_13
33. Wu X, Yan J, Wu Y, Zhang H, Mo S, et al. 2019. Proteomic analysis by iTRAQ-PRM provides integrated insight into mechanisms of resistance in pepper to *Bemisia tabaci* (Gennadius). *BMC Plant Biology* 19:270
34. Chatterjee A, Pandey S, Singh PK, Pathak NP, Rai N, et al. 2015. Biochemical and functional characterizations of tyrosine phosphatases from pathogenic and nonpathogenic mycobacteria: indication of phenyl cyclopropyl methyl-/phenyl butenyl azoles as tyrosine phosphatase inhibitors. *Applied Microbiology and Biotechnology* 99:7539–48
35. Zhang X, Yin F, Xiao S, Jiang C, Yu T, et al. 2019. Proteomic analysis of the rice (*Oryza officinalis*) provides clues on molecular tagging of proteins for brown planthopper resistance. *BMC plant biology* 19:30
36. Liu W, Meng L, Zhao W, Wang Z, Miao C, et al. 2022. Proteomic and metabolomic evaluation of insect- and herbicide-resistant maize seeds. *Metabolites* 12:1078
37. de Mello US, Vidigal PMP, Vital CE, Tomaz AC, de Figueiredo M, et al. 2020. An overview of the transcriptional responses of two tolerant and susceptible sugarcane cultivars to borer (*Diatraea saccharalis*) infestation. *Functional & Integrative Genomics* 20:839–55
38. Coppola V, Coppola M, Rocco M, Digilio MC, D'Ambrosio C, et al. 2013. Transcriptomic and proteomic analysis of a compatible tomato-aphid interaction reveals a predominant salicylic acid-dependent plant response. *BMC Genomics* 14:515
39. Bilgin DD, Zavala JA, Zhu J, Clough SJ, Ort DR, et al. 2010. Biotic stress globally downregulates photosynthesis genes. *Plant, Cell & Environment* 33:1597–613
40. Kerchev PI, Fenton B, Foyer CH, Hancock RD. 2012. Plant responses to insect herbivory: interactions between photosynthesis, reactive oxygen species and hormonal signalling pathways. *Plant, Cell & Environment* 35:441–53
41. Moustaka J, Moustakas M. 2023. Early-Stage detection of biotic and abiotic stress on plants by chlorophyll fluorescence imaging analysis. *Biosensors* 13:796
42. Shen W, Fu Y, Wang L, Yao Y, Zhang Y, et al. 2023. Transcriptomic analysis revealed that low-density aphid infestation temporarily changes photosynthesis and disease resistance but persistently promotes insect resistance in poplar leaves. *Forests* 14:1866
43. Foyer CH, Rasool B, Davey JW, Hancock RD. 2016. Cross-tolerance to biotic and abiotic stresses in plants: a focus on resistance to aphid infestation. *Journal of Experimental Botany* 67:2025–37
44. Al-Khayri JM, Rashmi R, Toppo V, Chole PB, Banadka A, et al. 2023. Plant secondary metabolites: the weapons for biotic stress management. *Metabolites* 13:716
45. Xue C, Yao J, Xue YS, Su GQ, Wang L, et al. 2019. PbrMYB169 positively regulates lignification of stone cells in pear fruit. *Journal of experimental botany* 70:1801–14
46. Kim Ji, Zhang X, Pascuzzi PE, Liu CJ, Chapple C. 2020. Glucosinolate and phenylpropanoid biosynthesis are linked by proteasome-dependent degradation of PAL. *New Phytologist* 225:154–68
47. He J, Liu Y, Yuan D, Duan M, Liu Y, et al. 2020. An R2R3 MYB transcription factor confers brown planthopper resistance by regulating the phenylalanine ammonia-lyase pathway in rice. *Proceedings of the National Academy of Sciences of the United States of America* 117:271–77
48. Wang Y, Sheng L, Zhang H, Du X, An C, et al. 2017. *CmMYB19* overexpression improves aphid tolerance in chrysanthemum by promoting lignin synthesis. *International Journal of Molecular Sciences* 18:619
49. An C, Sheng L, Du X, Wang Y, Zhang Y, et al. 2019. Overexpression of *CmMYB15* provides chrysanthemum resistance to aphids by regulating the biosynthesis of lignin. *Horticulture Research* 6:84
50. Chen K, Song M, Guo Y, Liu L, Xue H, et al. 2019. MdMYB46 could enhance salt and osmotic stress tolerance in apple by directly activating stress-responsive signals. *Plant Biotechnology Journal* 17:2341–55
51. Senani N, Bedouhene S, Houali K. 2023. Peroxidase activity as a biochemical marker of insecticide use in vegetables. *Acta Agriculturae Slovenica* 119(2):1–9
52. Wang Y, Zhang M, Du P, Liu H, Zhang Z, et al. 2022. Transcriptome analysis of pod mutant reveals plant hormones are important regulators in controlling pod size in peanut (*Arachis hypogaea* L.). *PeerJ* 10:e12965
53. Zhao X, Niu Y, Bai X, Mao T. 2022. Transcriptomic and metabolic profiling reveals a lignin metabolism network involved in mesocotyl elongation during maize seed germination. *Plants* 11:1034
54. López-Castillo LM, González-Leyzaola A, Díaz-Flores-Rivera MF, Winkler R, Wielsch N, et al. 2020. Modulation of aleurone peroxidases in kernels of insect-resistant maize (*Zea mays* L.; Pob84-C3R) after mechanical and insect damage. *Frontiers in Plant Science* 11:781
55. López-Castillo LM, Díaz Flores-Rivera MF, Winkler R, García-Lara S. 2018. Increase of peroxidase activity in tropical maize after recurrent selection to storage pest resistance. *Journal of Stored Products Research* 75:47–55
56. Hu Q, Min L, Yang X, Jin S, Zhang L, et al. 2018. Laccase GhLac1 modulates broad-spectrum biotic stress tolerance via manipulating phenylpropanoid pathway and jasmonic acid synthesis. *Plant physiology* 176:1808–23
57. Iqbal MJ, Ahsan R, Afzal AJ, Jamai A, Meksem K, et al. 2009. Multi-genetic QTL: the laccase encoded within the soybean Rfs2/rhg1 locus inferred to underlie part of the dual resistance to cyst nematode and sudden death syndrome. *Current Issues in Molecular Biology* 11:i11–i19
58. Katoch R. 2022. Nutritional quality of major forage grasses of Himalayan region. In *Nutritional Quality Management of Forages in the Himalayan Region*. Singapore: Springer. pp. 279–308. https://doi.org/10.1007/978-981-16-5437-4_10
59. Zhang L, Gu H, Gong D, Chang J. 2011. Research progress of cinnamyl alcohol dehydrogenase and its gene. *Acta Botanica Boreali-Occidentalia Sinica* 31:204–11
60. Jin S, Ren Q, Lian L, Cai X, Bian L, et al. 2020. Comparative transcriptomic analysis of resistant and susceptible tea cultivars in response to *Empoasca onukii* (Matsuda) damage. *Planta* 252:10
61. Zhu J, Zhang H, Huang K, Guo R, Zhao J, et al. 2023. Comprehensive analysis of the laccase gene family in tea plant highlights its roles in development and stress responses. *BMC Plant Biology* 23:129
62. Islam MT, Kudla-Williams C, Kar S, Londo JP, Centinari M, et al. 2022. Deciphering genome-wide transcriptomic changes in grapevines heavily infested by spotted lanternflies. *Frontiers in Insect Science* 2:971221
63. Wan J, Yi J, Tao Z, Ren Z, Otieno EO, et al. 2022. Species-specific plant-mediated effects between herbivores converge at high damage intensity. *Ecology* 103(5):e3647



Copyright: © 2023 by the author(s). Published by Maximum Academic Press, Fayetteville, GA. This article is an open access article distributed under Creative Commons Attribution License (CC BY 4.0), visit <https://creativecommons.org/licenses/by/4.0/>.